Title

Systematic optimization of an engineered hydrogel allows for selective control of human neural stem cell survival and differentiation after transplantation in the stroke brain.

Permalink

https://escholarship.org/uc/item/9t02j558

Authors

Moshayedi, Pouria
Nih, Lina R
Llorente, Irene L
et al.

Publication Date

2016-10-01

DOI

10.1016/j.biomaterials.2016.07.028

Peer reviewed

Systematic optimization of an engineered hydrogel allows for selective control of human neural stem cell survival and differentiation after transplantation in the stroke brain

Pouria Moshayedi[1†], Lina R. Nih[2†], Irene L. Llorente[1], Andrew R. Berg[1], Jessica Cinkornpumin[3], William E. Lowry[3], Tatiana Segura[2*], S. Thomas Carmichael[1*]

[1] Department of Neurology, David Geffen School of Medicine, University of California, Los Angeles, 635 Charles Young Drive, CA 90095, USA.

[2] Department of Chemical and Biomolecular Engineering, University of California, Los Angeles, 420 Westwood Plaza, CA 90095, USA.

[3] Department of Molecular Cell and Developmental Biology, University of California, Los Angeles, 710 Westwood Plaza, CA 90095, USA.

† These authors contributed equally to this work.

* Corresponding authors:

Professor S. Thomas Carmichael

Tel.: +1-310-206-9826; E-mail address: scarmichael@mednet.ucla.edu

Professor Tatiana Segura

Tel.: +1-310-206-3980; E-mail address: tsegura@g.ucla.edu

Abstract

Stem cell therapies have shown promise in promoting recovery in stroke but have been limited by poor cell survival and differentiation. We have developed a hyaluronic acid (HA)-based self-polymerizing hydrogel that serves as a platform for adhesion of structural motifs and a depot release for growth factors to promote transplant stem cell survival and differentiation. We took an iterative approach in optimizing the complex combination of mechanical, biochemical and biological properties of an HA cell scaffold. First, we optimized stiffness for a minimal reaction of adjacent brain to the transplant. Next hydrogel crosslinkers sensitive to matrix metalloproteinases (MMP) were incorporated as they promoted vascularization. Finally, candidate adhesion motifs and growth factors were systemically changed *in vitro* using a design of experiment approach to optimize stem cell survival or proliferation. The optimized HA hydrogel, tested *in vivo*, promoted survival of encapsulated human neural progenitor cells (iPS-NPCs) after transplantation into the stroke core and differentially tuned transplanted cell fate through the promotion of glial, neuronal or immature/progenitor states. This HA hydrogel can be tracked in vivo with MRI. A hydrogel can serve as a therapeutic adjunct in a stem cell therapy through selective control of stem cell survival and differentiation in vivo.

1. Introduction

Stroke is the leading cause of long-term disability [1]. There are no therapies that promote recovery in this disease. New strategies aimed at enhancing post-stroke brain plasticity have utilized trophic factors, stem cell therapies or a combination of the two. However, their clinical translation has been limited because of the short half-life and undesirable systemic effects of injected growth factors [2, 3] and poor survival of transplanted cells [4], partly due to the abrupt withdrawal of adhesive support and the inflammatory environment of the damaged brain [5]. Although there are many protocols to differentiate *in vitro* stem/progenitor cells to desired fates, *in vivo* these protocols are either not possible or fail to differentiate the cells to the same extent. The lack of a successful medical therapy that promotes long-term recovery in stroke imposes a substantial clinical and economic burden, indicating the need for a novel therapeutic solution.

Recent advances in tissue engineering have developed injectable hydrogels that can serve both as a protective vehicle for cells and a depot release platform for trophic factors, with distinct synergistic advantages of both strategies. Cell-loaded hydrogels provide structural support that not only directly promote the survival of encapsulated cells [6], but also promote cell infiltration from the surrounding parenchyma [7] and reduce the glial scar and inflammation at the ischemic border [8, 9]. Similarly, local drug delivery from injectable hydrogels can achieve sustained [3, 10, 11] or sequential delivery [12] in a time- and space-controlled manner, while enhancing protein stability, diffusion distance and *in vivo* bioactivity [11]. Polymer-based hydrogels are highly customizable as their composition can be modified to adapt to the host tissue. For example, a simple alteration of the polymer length, the crosslinking points and/or the scaffold mesh size can modulate gel stiffness, nutrient diffusion, and even cell motility [13]. Recent studies have shown that a wide variety of chemical, mechanical and spatial cues can be incorporated into cell–material interactions to ultimately allow for greater control over cell behavior [14].

Hyaluronic acid (HA) gels are appealing choices for cell encapsulation in a transplant approach. HA is abundantly found in the brain, particularly in the endogenous environment for neural progenitor cells (NPCs) [15] and it is both a biocompatible and bioresorbable material that allows cells to degrade it as they spread within the gel [16]. We have previously reported a hyaluronic acid hydrogel crosslinked *in situ* via thiol/acrylate Michael type addition for human

induced pluripotent neural precursor (iPS-NPC) culture *in vitro,* which demonstrated biocompatibility after transplantation *in vivo* [13].

Stroke offers a unique opportunity for a tissue engineering neural repair therapy. After initial cell death in stroke, the clearance of debris in the lesion leaves a compartmentalized cavity that can accept a large volume transplant without further damaging the surrounding healthy parenchyma [17]. This stroke cavity is situated directly adjacent to the peri-infarct tissue, the region of the brain that undergoes the most substantial repair and recovery, meaning that any therapeutic delivered to the cavity will have direct access to the tissue target for repair [2]. Although utilizing a hydrogel material to promote differentiation of transplanted stem cells is a logical next step, no published study has shown substantial differentiation or differential control over post-transplantation cell fate. We developed a hydrogel material that can control transplanted human neural progenitor cell fate *in vivo* after the injection through the modulation of adhesive and trophic signals delivered from the scaffold. We show that the material can be optimized *in vitro* to result in either maintenance of the progenitor state or differentiation towards different central nervous system fates *in vivo*. Our findings mark the first time a hydrogel has been engineered to control transplanted human stem/progenitor cell fate *in vivo* utilizing *in vitro* findings.

2. Materials and Methods

2.1. Cell culture

Induced pluripotent stem cells (iPS) were generated from human fibroblasts and characterized [18] under approved protocols from the UCLA ESCRO. NPCs were differentiated from iPS through formation of neural rosettes and maintained in culture [19]. On the day of transplantation human iPS-NPCs were harvested by TrypLE treatment (3-5 minutes; Life Technologies), centrifuged at 300 g for 5 minutes, re-suspended in maintenance culture medium and kept on ice. Cell viability throughout transplantation process remained above 95%-97% as determined by Trypan blue exclusion method. Animal origin-free products were used for the cell culture.

2.2. Hyaluronic acid modification

Hyaluronic acid (60,000 Da, Genzyme, Cambridge, MA) was functionalized with an acrylate group using a two-step synthesis as previously described [20]. After dissolving the HA (2.0 g, 5.28 mmol) in water, it was reacted with adipic dihydrazide (ADH, 18.0 g, 105.5 mmol) in the presence of 1-ethyl-3-(dimethylaminopropyl) carbodiimide hydrochloride (EDC, 4.0 g, 20 mmol) overnight at a pH of 4.75. The hydrazide-modified hyaluronic acid (HA-ADH) was purified with decreasing amounts of NaCl (100, 75, 50, 25 mmol) for 4 hours each via dialysis (8,000 MWCO). The solution was then purified via dialysis (8000 MWCO) in deionized water for 2 days and lyophilized. The HA-ADH was re-suspended in 4-(2-hydroxyethyl)-1-piperazine ethane-sulfonic acid (HEPES) buffer (10 mM HEPES, 150 mM NaCl, 10 mM EDTA, pH 7.4) and reacted with N-acryloxysuccinimide (NHS-AC), 1.33 g, 4.4 mmol) overnight. After purification via dialysis as described earlier, the acrylated HA (HA-AC) was lyophilized. The product was analyzed with 1H NMR (D_2O) and the degree of acrylation (14.9%) determined by dividing the multiplet peak at δ = 6.2 (cis and trans acrylate hydrogens) by the singlet peak at δ = 1.6 (singlet peak of acetyl methyl protons in HA). This gel was chosen because of its biocompatibility with human tissue, as it is constituted of naturally occurring brain extracellular matrix constituents. The mechanical properties of this gel are similar to those of normal brain. HA has been shown to promote angiognesis in a mouse model of skin wound healing [21, 22]. Biotin was then introduced to HA-AC using sulfo-NHS–LC–biotin (NHS–biotin). NHS–biotin (100mg) was added as a solid to a solution of HA–AC (300 mg; 3 mg/mL in PBS; pH 7.4) as previously described [22]. The reaction proceeded for 16 hours at room temperature with stirring. The reaction product was then purified by dialysis (MWCO 14,000) against distilled water for 24 hours. The final purified product was

lyophilized and stored at 4°C until used.

2.3. Heparin modification

Heparin Carboxylic acid groups (Alfa Caesar, Ward Hill, MA) were functionalized with thiol groups by dissolving 2 mg/mL of heparin in PBS. To this solution, EDC, NHS, and an excess amount of cysteamine were added. The pH of the reaction mixture was adjusted to 4.75 and the reaction was allowed to continue overnight with stirring at room temperature. DTT was then added to reduce the oxidized disulfide groups in order to release thiol groups. This solution was allowed to react overnight at pH 7.5 and then adjusted to pH 3.5 by the addition of 1.0 N HCl. Next, the reaction solution was dialyzed and lyophilized. The amount of the thiol group attached to heparin was measured using the molar absorptivity of Ellman's reagent at 412 nm.

2.4. Gelation

Lyophilized acryl hydrazide hyaluronic acid was dissolved in 4-(2-hydroxyethyl)-1- piperazine ethane-sulfonic acid (HEPES, 0.3 M) buffer for 15 minutes at 37°C for the *in vitro* experiments, and 20 minutes at room temperature for the *in vivo* injections. The appropriate concentration of Ac-GCGYGRGDSPG-NH2 adhesion peptide (RGD, Genscript, Piscataway, NJ), Ac-GCGYGYIGSR-NH2 (YIGSR, Genscript), Ac-IKVAVGYGCG-NH2 (IKVAV, Genscript) was dissolved in 0.3 M HEPES and added to the dissolved HA-AC and allowed to react for 20 minutes. For *in vitro* studies gel culture media, iPS-NPCs (3,000 cells/µL final concentration), were then added. Heparin and growth factors were then added to the gel precursor solution, before the addition of a MMP-degradable peptide cross-linker (Ac- GCRDGPQGIWGQDRCG-NH2, Genscript), dissolved in 0.3 M HEPES. For in the *in vitro* experiments, 5 µL of this solution was pipetted onto, and sandwiched between two Sigmacote (Sigma-Aldrich) functionalized glass coverslips and placed in an incubator for 30 minutes at 37°C to gel. For injections into stroke brains, the precursor was loaded into the Hamilton syringe directly after mixing in the desired cross-linking peptide. The gel remains liquid for at least 10 minutes after mixing, allowing it to be injected.

2.5. Rheometry

Gels without cells were made as described above and cut to size using a 8.0 mm biopsy punch. The modulus was measured with a plate-to-plate rheometer (Physica MCR 301, Anton Paar,

Ashland, VA) using a 8 mm plate with a frequency range of 0.1-10 rad/s under a constant strain of 1% at 37°C. An evaporation blocker system was used to keep the gel from dehydrating during the test. Addition of iPS-NPCs to the HA gel did not change mechanical properties of gels shortly after gelation (Figure 1; [54])

2.6. Cell survival in vitro

Cell survival was measured using the CyQUANT cell proliferation assay kit (Invitrogen). Gels were washed twice in 1x PBS and frozen in a -80 freezer at days 1 and 7 after gel gelation. After thawing the gels at room temperature, they were degraded by incubation in TrypLE express (Invitrogen) at 37°C for 15 minutes. The cells were isolated by centrifuging the solution at 250 g for 5 minutes and re-suspended in 200 µL of the CyQUANT GR dye/cell-lysis buffer. After 5 minute incubation, the fluorescence was read using a plate reader at 480 nm.

2.7. Flow cytometry

Gels at day 1 or 7 after gelation were rinsed in 1x PBS and degraded by pipetting the gel up and down via a 1000 µL pipette. The solution was spun at 250 g for 10 minutes and re-suspended in BD Cytofix (Becton Dickinson, New Jersy) for 30 minutes at room temperature. After spinning down at 250 g for 5 minutes, samples were re-suspended in 1x PBS + 1% bovine serum albumin (BSA, Fisher Scientific) + 0.2% saponin (Sigma-Aldrich) for 15 minutes at room temperature. Antibodies were then added to the solution for 30 minutes at room temperature. Following a spin at 250 g for 5 minutes, the samples were re-suspended in 1% paraformaldehyde for Fluorescence Activated Cell Sorting (FACS). Analysis was performed using a FACScan X (BD Bioscience, San Jose, CA) and the data was analyzed using FLOWJO (Version 10.0.7; Tree Star Inc, Ashland, OR). Triplicates were done for each condition with 3000 events/sample. The Dcx samples were gated to contain the positive signal peak.

2.8. Design of experiments

JMP software (SAS, Cary, NC) was used to generate the gel conditions and to analyze the subsequent data. A surface response methodology (RSM) setup was used to vary the ligands of interest within a specific concentration range using a central composite inscribed design (CCI). For each iteration, a response surface methodology experiment was developed in which each variable factor was given a defined range (µM) to be modulated within. Here, the Central

composite on face, a specific RSM statistical design was chosen, as this system enabled us to test the end points of each factor. Data from the cell survival assay for each condition recommended was inputted back into the software. The data was analyzed via a least squares regression model to determine significance of the factors and plot the predicted response surface. Each condition was done in triplicate and data from gels at day 7 were normalized to gels from the same condition at day 1 to account for any differences in the numbers of cells encapsulated in the gel precursor solution.

2.9. Inducing stroke and transplantation

The procedures involving animals and human cells were performed in accordance with National Institutes of Health Animal Protection Guidelines and approved by the UCLA Chancellor's Animal Research Committee as well as the UCLA Office of Environment Health and Safety. A cortical model of photothrombotic stroke was produced in 2-month-old male C57BL/6 (Jackson Laboratory, Bar Harbor, ME) or Nod-Scid-gamma (NSG) mice (Jackson Laboratories). Mice were anesthetized and maintained with 2% isoflurane in N2O:O2 (2:1). Stroke was produced with a light-sensitive dye in a photothrombotic approach as previously described [23]. Briefly, mice were positioned in a stereotaxic instrument and administered Rose Bengal (10 mL/gr from 10 mg/mL solution, i.p.). A 2 mm diameter region of the closed skull was illuminated with a white light for 15 minutes. Temperature was maintained at 37±0.5 °C (RightTemp™, Kent Scientific, Torrington, CT). The mouse was allowed to recover in its home cage. Seven days after stroke, when the necrosis of infarcted tissue at the stroke core has made a potential space for incorporating injected volumes [24], cells, gel or cells encapsulated in gel were injected into the core of stroke. Cells were spun at 300 g for 5 minutes and re-suspended in PBS or HA gel premix (including gel ingredients without cross-linker) at 50,000 cells/µL (or 25,000 cells/µL for the experiment studying effects of cell concentration on HA gel resorption). To inject cells encapsulated in gels or gels alone the cross-linker was added and thoroughly mixed immediately before the gel mixture was withdrawn into a 25 µL Hamilton syringe (Hamilton Company, Reno, NV). Injections were conducted through a 30 G Hamilton needle into a point 0.6 mm below the surface of the brain. Two µL of volume, was injected at 0.3 µL/mL rate. To study cell survival in C57BL/6 mice, animals were immunosuppressed with Tacrolimus (Cell Signaling, Danvers, MA). Four intraperitoneal injections of Tacrolimus (3mg/kg; dissolved in DMSO) were delivered for total of 4 days starting 2 days before implanting minipumps. At the time of the stroke surgery, 3 mg/kg/day

Tacrolimus (dissolved in 50% DMSO, 15% ethanol and 35% distilled water) was infused from a minipump (Model 1002; DURECT Corporation, Cupertico, CA). Minipumps were implanted subdermally between the scapulae and changed every two weeks. Upon minipump extraction a successful infusion of Tacrolimus was ensured by checking for any remaining Tacrolimus solution. Additional subcutaneous injections of tacrolimus were administered on the day of pump replacement since it takes ~12hrs for miniosmotic pump to start infusion.

2.10. Magnetic Resonance Imaging of mice

Mice were anesthetized and placed in a small animal MRI (7T, Bruker BioSpin, Fremont, CA) 9 weeks after stroke. Respiratory rate was monitored throughout the procedure and body temperature was maintained at 37±0.5°C. A T2-weighted image set was acquired with the following parameters: rapid acquisition relaxation enhancement factor 8, repetition time 5300 milliseconds, echo time 15.00 milliseconds with an in-plane resolution of 0.039_0.039_0.50 mm with 13 contiguous slices. The MRI images were exported by the software ParaVision 5.1 (Bruker BioSpin, Fremont, CA) into a high-resolution file format (2DSEQ) and volumetric measurements were performed in ImageJ (National Institute of Health, Bethesda, MD). Gel area, which was represented as a T2 hyperintense signal in T2 sequence images, was quantified in all MRI images cut through lesion areas.

2.11. Tissue processing

Infarct size was determined 3-5 days after stroke by staining with a 2% triphenyl tetrazolium chloride (TTC; gr/mL, made in PBS; Sigma-Aldrich, St Louis, MO) solution for 40 minutes at 37°C. The brain was then cut in 1 mm sections using a mouse Brain Matrix (Zivic Instruments, Pittsburgh, PA) and imaged using a stereomicroscope. The same preparation was used to quantify hydrogel volume one day after injection. For immunohistochemical studies mice were euthanized at 2 weeks or 6 weeks after cell or gels or cells in gels injections and perfused with 4% paraformaldehyde (Fisher Scientific, Pittsburgh, PA; in PBS, pH: 7.4) and cryoprotected in sucrose for 48 hours. Brains were cut on cryostat at 16 µm intervals and mounted on gelatin-coated Superfrost® slides (Fisher Scientific).

2.12. Immunohistochemistry

For transplant cell quantification, tissue sections were stained for HuNu, a human-specific nuclear antigen, using avidin-biotin complex (ABC) amplification (VECTASTAIN® Elite® ABC Kit-

Mouse IgG, Vector Laboratories, Burlingame, CA) and 3,3'-diaminobenzidine (DAB) labeling (ImmPACT™ DAB, Vector Laboratories) with blocking of endogenous biotin (Lab Vision™, Thermo Fisher Scientific, Fremont, CA). Immunofluorescence was performed using primary antibodies (Table S1) incubated overnight. HA gels were labelled for the biotin, and this was visualized using streptavidin tyramide signal amplification (TSA™, Life Technologies). All antibodies utilized are in Supplementary Table [54].

2.13. Tissue analysis

Stroke volume was quantified in TTC-stained 1 mm brain sections by summing stroke areas multiplied by inter-slice distance of 1 mm. To measure vessel density inside transplants, slides were scanned with laser scanning confocal microscopy (C2 Series, Nikon Instruments Inc., Melville, NY), total length of vessels was measured by ImageJ and divided by volume of transplant computed as area multiplied by the section thickness. For colocalization studies the percentage of tissue volume in which GFP marker colocalized with a second marker was calculated in confocal image stacks using IMARIS software (Bitplane, South Windsor, CT).

2.14. Statistics

Tests were analyzed blindly to experimental condition. Animals were randomly assigned to control and treatment groups. Power analysis tool (Statistical Solutions LLC, Cottage Grove, WI) was employed to calculate sample size with the expected variance and changes in predicted proliferation and differentiation rates based on preliminary data. Data for each group/time-point comprise 4-7 individual animals. Data is presented as mean ± SEM. Multiple comparisons ANOVA with Bonferonni or Dunnet (when compared against control) post-hoc tests were performed on data. If data did not fit into a normal distribution then tests appropriate for non-parametric variables, such as Mann-Whitney test (for comparison between two groups) or Kruskal-Wallis test (for comparison among three or more groups) followed by Dunn post-hoc test, were employed.

3. Results

3.1. Optimizing mechanical properties of HA gel in vivo

With the goal of injecting this gel into the stroke cavity, we identified the mechanical properties and gelation conditions that allowed the gel to fully flow into and fill the stroke cavity before gelation. HA gels with three different stiffness levels 100, 350 and 1000 Pa were injected in the stroke cavity (Figure 1A, 1B*i-iii*) one week after the stroke onset. This time point of injection was chosen as it corresponds to a period in which cell death in stroke is complete, and a clinical window in which patients might receive a stem cell/hydrogel therapy [2]. Twenty-four hours after the injection, both the intracerebral volume of gel and the remaining damaged tissue in the stroke area were measured. Both the 350 Pa and 1 kPa HA gels had significantly more volume of gel remaining in the brain (Figure 1B*vi*). However, the injected 350 Pa gel, which matches the mechanical properties of brain cortex [25], was associated with the lowest remaining volume of infarcted tissue (Figure 1B*vii*), thus occupying the stroke cavity with the highest efficiency and establishing the most optimum gel-tissue interface. This greater expansion of the 350Pa gel and more complete occupation of the stroke cavity could be described because this gel matches the brain tissue's stiffness and leads to the gel conforming to stroke cavity boundaries and expelling, or compressing infarcted tissue. Therefore, the 350 Pa gel was chosen for the rest of the study.

3.2. Crosslinker sensitivity to MMPs in vivo

Hydrogel cross-linkers influence gel stability and degradation processes [26]. Stroke induces degradative enzyme, such as matrix metalloproteinaes (MMPs) [25], that may serve to modify an injected hydrogel. Crosslinking motifs sensitive to MMPs were incorporated in the gel and compared to the hydrogel cross-linked with motifs insensitive to the enzymes. Two weeks after gel injection, mice were sacrificed and brain sections were stained for collagen (Figures 1B*iv*, *v*), a component of the vascular basement membrane [27]. While very few vessels were found in the MMP-insensitive condition (Figure 1B*iv*), a significantly increased vascular in-growth was observed in the MMP-degradable gel (Figures 1B*v*, *viii*).

3.3. DOE approach to optimize the concentration of adhesion motifs and growth factors in vitro

Incorporating biochemical cues within hydrogel materials used for stem cell transplantation is an ideal approach to control survival and differentiation. However, there is a disconnect between the studies performed *in vitro*, which often utilize soluble differentiation cocktails to achieve differentiation, and the gels that are used *in vivo*. This is because either the precise control over an *in vitro* biochemical environment is not plausible *in vivo*, or a different *in vivo* differentiation outcome is observed despite of delivering the same *in vitro* growth factor cocktail. Our group recently showed that a statistical Design of Experiment (DOE) approach [21] can be used to optimize the concentration of adhesion motifs derived from laminin (IKVAV and YIGSR) and fibronectin (RGD) to promote the *in vitro* survival of iPS-NPCs and demonstrated that the optimal condition promoted neuronal differentiation [13]. Here we utilize the same DOE approach to optimize the concentration of brain-derived neurotrophic factor (BDNF) and bone morphogenic protein-4 (BMP-4) (both of which have potent effects on NPC differentiation [28]) to promote survival *in vitro* and differentiation to different lineages *in vivo*. Human iPS-NPCs were used in these studies as these are a viable therapeutic candidate for a stem cell therapy in stroke [29].

In order to increase retention of the growth factors by the hydrogel matrix *in vivo*, heparin was introduced to the HA backbone. Two separate DOE optimizations were performed using soluble or heparin-bound growth factors. For each DOE optimization experiment 5 different concentrations of BDNF or BMP-4 (0, 50, 100, 150 or 200 ng/mL) were combined into twelve different gel conditions (Figure 1C*i* and 1D*i*) while keeping one single peptide motif (RGD: 300 µM) constant. The soluble forms of BDNF and BMP-4 resulted in an optimal combination for the greatest (BDNF: 200 ng/mL, BMP-4: 0) and least cell survival (BDNF: 0 ng/mL, BMP-4: 26.52 ng/mL; Figure 1C*ii*). As expected the bound forms of growth factors (GF) resulted in a different optimal formulation for the greatest survival labeled as "GF Max" (BMP-4: 37.22 ng/mL; BDNF: 0 ng/mL) and the least survival labeled as "GF Min" (BDNF: 200 ng/mL; BMP-4: 155.28 ng/mL, Figure 1D*ii*). Differences between soluble and bound growth factors have been previously observed and can be attributed to different signaling responses for bound growth factors [30]. All conditions had a cell survival equal to or greater than the cell number found at day 1 after iPS-NPC encapsulation within the hydrogels.

This approach optimized growth factors and adhesion peptides separately. A final stage of optimization consisted of combining both optimal formulations for growth factors ("GF Max", "GF Min") and the optimal regimen for peptides ("Pept Max": RGD: 100 µM, IKVAV: 48 µM, YIGSR: 300 µM and "Pept Min": RGD: 0, IKVAV: 100 µM, YIGSR: 45 µM from ref. [21]) described as GF Max + Pept Max = HA Max, and GF Min + Pept Min = HA Min (Figure 1F). HA Nopt gel remained as a non-optimized interim control gel with equimolar concentrations of adhesion motifs and no GF. These conditions proposed by DOE were then tested *in vitro* to confirm the effects on survival, spreading and differentiation of encapsulated iPS-NPCs using immunofluorescence staining and flow cytometry (Figure 1E*i-iv*). HA Max, the gel optimized by DOE to promote cell survival, was associated with significantly increased cell survival, axonal sprouting, and expression of a neuronal differentiation marker, doublecortin (Dcx) [31] compared with HA Min and a non-optimized control gel with only RGD motif. Interestingly the HA Min condition, designed to lower cell survival in DOE approach, showed a statistically lower cell survival and differentiation than the RGD only control gel and the GF Min condition, respectively (Figure 1E*i*, *iii*). Therefore the HA gel formulations predicted by DOE approach showed consistent *in vitro* results.

3.4. Effects of gel composition on brain tissue adjacent to the stroke

This step-by-step hydrogel optimization led to four candidates for *in vivo* testing: 1) an empty HA gel without any adhesion peptide or growth factor (HA), 2) a non-optimized gel with equimolar concentrations of RGD, IKVAV and YIGSR peptides (100 µM each) and no growth factors as a control for DOE optimization process (HA Nopt), 3) a gel with both optimized concentrations of growth factors and of peptides for a maximum cell survival *in vitro* (HA Max) and 4) a comparator gel with the same growth factors and adhesion motifs but with concentrations to result in a minimized cell survival *in vitro* (HA Min). A first *in vivo* experiment aimed at evaluating the effect of the different gel conditions in the absence of encapsulated cells on the activation of host tissue microglia and astrocytes, as HA hydrogels may induce an inflammatory and astrocytic reaction to an injected scaffold [15]. C57BL/6 mice were injected with the four different gel conditions directly into the stroke cavity one week after the stroke onset and sacrificed two weeks later. Brain sections were stained for GFAP (astrocytes) and Iba1 (microglia) and

compared with a non-injected stroke condition as a control. No significant difference was observed among all the conditions (Figure 2; [54]), indicating that none of the HA groups induced a greater inflammatory or astrocytic response than the stroke insult itself.

3.5. HA gel degradation and angiogenesis

Timely degradation of bioscaffolds is of paramount importance in tissue engineering. To determine the contribution of transplanted iPS-NPCs vs. host tissue in degradation of HA gels over time, the gel optimized for highest cell survival, spreading and differentiation, HA Max, was chosen. The biotin-tagged gel was loaded with either 50,000 or 100,000 iPS-NPCs prior to transplantation into the stroke area of immunodeficient NSG mice one week after stroke. Two and six weeks later, the results showed that the gel loaded with 100,000 cells lost substantial volume between the two time points (Figure 2A, B) while the gel loaded with 50,000 cells remained relatively intact for as long as six weeks (Figure 2C). The same observation was made with pharmacologically immunosuppressed C57BL/6 mice to mimic cell therapy for stroke in a clinical setting (data not shown). A T2 MRI sequence was used in these mice to quantify the remaining gel volume at nine weeks post-transplantation *in vivo*. HA hydrogels are visible on T2 MRI, due to their hydration shortening the T2 relaxation time [3]. The addition of 100,000 cells significantly decreased the gel volume compared with a cell-free gel (Figure 2D-J), suggesting that encapsulated cells, rather than the host brain tissue, are involved in the hydrogel breakdown. This breakdown may also be through the of infiltration adjacent brain tissue, such as the vasculature [15]. Fluorescent staining of vessels (CD31) revealed the presence of an extended vascular network within the gel as early as 2 weeks post-injection, displaying a close interaction with encapsulated iPS-NPCs (Figure 2K-O). The same observation was made in the three other HA conditions. No significant difference in measured vascular density was observed between gel transplant groups (data not shown).

3.6. Effects of HA gel composition on human iPS-NPC proliferation and differentiation in vivo

To test the effect of the four distinct gels on iPS-NPC proliferation and differentiation after stroke, iPS-NPCs were transplanted into the stroke cavity of immunodeficient NSG mice 7 days

after stroke. The NSG mouse strain was chosen to minimize the effects of host inflammation on *in vivo* cell proliferation and differentiation, as well as cell-scaffold interactions. Brain sections were stained for human nuclear antigen (HuNu) and the proliferation marker Ki67 at two and six weeks after transplantation, and double positive cells were counted (Figure 3A,B). The HA Max condition was associated with a significantly increased proliferation at two weeks compared with all the other conditions, before this level of proliferation decreased, showing no significant difference at the six week time point across gel transplant groups. Interestingly the six week time point coincides with gel degradation (Figure 2B) that would naturally terminate the pro-survival effect of HA Max gel on encapsulated cells.

iPS-NPC differentiation was studied by co-staining cells with SOX2 and NF200, expressed by immature neural precursors [32] and neurons [33], respectively. Notably all iPS-NPCs express SOX2 upon differentiation from iPS cells *in vitro* (data not shown), consistent with its known role in neural precursor function [19]. Non-encapsulated cells (No HA condition) were found to retain significantly higher levels of SOX2 expression compared to the conditions in which iPS-NPCs were transplanted within a hydrogel (Figure 3B) In addition iPS-NPCs transplanted in HA Nopt gel had a significantly increased co-labeling with NF200 compared with other groups, indicating a neuronal phenotype. In all transplant conditions iPS-NPCs did not express Oct4, a marker of stem cell pluripotency, indicating that there was not a de-differentiation across groups (data not shown). These findings indicate that encapsulation in any type of HA gel promotes differentiation away from the progenitor state after transplantation and this differentiation can be further directed towards neuronal cells with equimolar concentration of adhesive peptides in the absence of growth factors. Interestingly, the HA Max did not promote neuronal differentiation (Figure 3A, B) even though it contains BDNF [34] and BMP4 [35], growth factors that are associated with neuronal differentiation. This finding indicates that *in vivo* differentiation is more complex and multifactorial than expected.

To further study the effect of HA gels on glial differentiation as an alternative to neuronal differentiation of iPS-NPCs, tissue sections were stained for GFAP, expressed by both immature and mature astrocytes as well as NPCs, and S100b, mainly expressed by mature astrocytes [36] (Figure 4A). The ratio of GFP cells expressing only GFAP or both GFAP and S100b was quantified (Figure 4B). iPS-NPCs encapsulated in HA Max gels had a significantly increased

expression of both GFAP and S100b markers compared with the other groups. In our experimental paradigm S100b staining is more confined to astrocyte identity in contrast to GFAP staining, associated with both astrocytes and also reported in NPCs. To distinguish between astrocytic differentiation vs. remaining in a precursor state, the ratio of GFP-GFAP-S100b over GFP-GFAP revealed that the majority of GFP cells expressing GFAP also express S100b. This confirms that encapsulation in HA Max gels promotes astrocytic differentiation of iPS-NPCs within the stroke cavity.

3.7. Effects of HA gels on cell survival in vivo

Previous studies have indicated poor cell survival when directly injected into or near the stroke cavity [37]. Yet, the stroke cavity is an attractive clinical transplant site because it is a cavity and can accept a large volume injection [3] and because it is directly adjacent to the site of the most substantial plasticity and recovery after stroke, the peri-infarct tissue [38]. In the preceding experiments, NSG mice were used so that prolonged immunosuppressive regimens would not be necessary and the focus would be on the hydrogel effects on transplant cell differentiation. However, the deficient immune system of NSG mice allowed iPS-NPC survival equally in encapsulated and non-encapsulated cells (Figures 3A and 4A, also quantified cell number; data not shown) likely because the inflammatory insult on transplanted cells was too weak to require protective effects of growth factors and adhesion motifs on graft survival. To study pro-survival effects of HA gels in a condition mimicking clinical situations we used single agent immunosuppression, an approach used in human stem cell transplant trials [39], in C57Bl/6 wild type mice. Using GFP fluorescence quantification we found that encapsulating iPS-NPC in HA Max gel promoted survival two weeks after transplantation into the stroke cavity compared with non-encapsulated cells that appeared in very low numbers (Figure 3C). This indicates that in addition to controlling cell differentiation, HA gels promote survival in the early period after transplant.

4. Discussion

HA hydrogels promote differential maturation of neural progenitors *in vivo* within the stroke cavity, enhance survival of transplanted cells and represent a therapeutic approach that can be tracked *in vivo* with MRI. When directly injected into stroke (No HA condition) most iPS-NPCs retained SOX2 expression, a marker of immature neural progenitor cells [32]. iPS-NPCs preferentially differentiated into neurons when they were transplanted within an HA gel that contained fibronectin and laminin peptide motifs in maximal concentrations (HA Nopt). An HA gel with peptide motifs and BMP4 and BDNF growth factors optimized *in vitro* for survival and proliferation promoted astrocytic differentiation *in vivo*. Both astrocyte and neuronal differentiation of transplanted neural progenitor cells has been suggested as a potential therapy in brain diseases [29] indicating that modulation of progenitor cell differentiation toward either lineage may have clinical utility. This is the first report of selective control of neural progenitor cell differentiation *in vivo* after transplantation in stroke. These studies indicate that hydrogel scaffolds can be used to tune the differentiation of early progenitor cells toward distinct cell types, and provide flexible derivation of a particular neural repair therapy within the brain itself. Furthermore, this hydrogel scaffold/stem cell transplant approach promotes transplant survival within the stroke cavity, an avascular and inflamed tissue environment that is nonetheless a good site for a transplant therapy.

This study brings a deeper understanding of the environmental cues that dictate neural progenitor differentiation into specialized cells. All HA conditions were associated with cell differentiation to some extent, implying that the presence of the polymer scaffold itself guided cell exit from the multipotent progenitor stage independently of the addition of extracellular matrix cues or trophic factors. A second level of cell signaling further specifying a differentiation route is then seen in the unique cell fate associated with each HA condition, indicating that if the scaffold does not selectively engage a specific pathway, the gel composition does, highlighting the importance of the choice and combination of these cues and growth factors to optimize the hydrogel for the desired effect. Here, a non-optimized hydrogel (HA Nopt) characterized by an equimolar concentration of adhesion peptides promoted the formation of neurons, while an optimized gel for a maximized *in vitro* survival (HA Max) induced the *in vivo* state an early proliferation and formation of astrocytes. In a similar observation the pro-survival effect, an HA-

methylcellulose-based hydrogel was coupled with differentiation of human oligodendrocyte progenitor cells towards astrocytic phenotypes following transplantation into spinal cord injury [40]. Interestingly, the gel that produced minimized *in vitro* survival (HA Min) minimized neuronal differentiation *in vivo*. These results suggest that altering NPC proliferation and survival prevents cells from completing their differentiation to neurons.

Engineering a 3D biomaterial to culture and transplant cells enabled us to create a complex matrix environment by keeping the hydrogel platform and cell type constant across conditions while systematically varying peptide motifs and growth factors, highlighting the tunable characteristics of bioengineered synthetic matrices. Since advances have been made to improve the trophic abilities of engineered hydrogels to promote brain tissue regeneration, many recent combinatorial strategies have demonstrated the synergistic benefits of combining stem/progenitor cells and matrix [6, 41]. However, the majority of these studies have attempted to maximize the benefit of combination therapies by either changing one unique aspect of the therapy while maintaining the other elements constant [42, 43], by using a "presence/absence" binary evaluation of the matrix component [8, 44], or by picking random concentrations (usually equimolar) for all the factors tested [42, 45]. The use of DOE allows systematic alteration of multiple components of the hydrogel to determine outcome characteristics for further *in vivo* testing.

Tissue engineering in regenerative medicine requires overcoming complex control issues on two levels. The transplant itself exhibits a complex interaction with the recipient tissue and with adjoining transplant cells. Second, the recipient tissue has a complex structure and cell composition that makes tissue replacement challenging. Recently, studies have addressed transplant survival along with differentiation and repair of the recipient tissue with a data-driven statistical approach to optimize the gel composition to promote tissue repair. Many of these investigations have transitioned from *in vitro* to *in vivo* in the tissue-engineering field of organs such as retina [46], skin [47], liver [48], digestive tract [49], ear [50], pancreas [51], lungs [52] and skeletal muscle [53]. However the systematic development of a bioengineered scaffold for the brain with DOE studies has been rarely pursued past the *in vitro* stage [21, 22]. This work provides the first evidence supporting the multi-factorial cell/hydrogel/DOE approach that combines mechanical, biochemical and trophic factors to 1) systematically modify multiple factors at the same time, 2) identify the specific combination that promotes the desired cell behavior and 3) selectively control

the *in vivo* distinct cell fate of transplanted cells. This works highlights the importance of interdisciplinary collaborations between engineers, clinicians, and biologists in the development of innovative cell transplantation therapies after stroke.

5. Acknowledgments

6. References

[1] Go AS, Mozaffarian D, Roger VL, Benjamin EJ, Berry JD, Blaha MJ, et al. Heart disease and stroke statistics--2014 update: a report from the American Heart Association. Circulation. 2014;129:e28-e292.

[2] Carmichael ST. Emergent properties of neural repair: Elemental biology to therapeutic concepts. Annals of neurology. 2016.

[3] Cook DJ, Nguyen C, Chun HN, I LL, Chiu AS, Machnicki M, et al. Hydrogel-delivered brain-derived neurotrophic factor promotes tissue repair and recovery after stroke. Journal of cerebral blood flow and metabolism : official journal of the International Society of Cerebral Blood Flow and Metabolism. 2016.

[4] Parr AM, Tator CH, Keating A. Bone marrow-derived mesenchymal stromal cells for the repair of central nervous system injury. Bone Marrow Transplant. 2007;40:609-19.

[5] Carpentier PA, Palmer TD. Immune influence on adult neural stem cell regulation and function. Neuron. 2009;64:79-92.

[6] Zhong J, Chan A, Morad L, Kornblum HI, Fan G, Carmichael ST. Hydrogel matrix to support stem cell survival after brain transplantation in stroke. Neurorehabil Neural Repair. 2010;24:636-44.

[7] Yu H, Cao B, Feng M, Zhou Q, Sun X, Wu S, et al. Combinated transplantation of neural stem cells and collagen type I promote functional recovery after cerebral ischemia in rats. Anatomical record. 2010;293:911-7.

[8] Hoban DB, Newland B, Moloney TC, Howard L, Pandit A, Dowd E. The reduction in immunogenicity of neurotrophin overexpressing stem cells after intra-striatal transplantation by encapsulation in an in situ gelling collagen hydrogel. Biomaterials. 2013;34:9420-9.

[9] Ju R, Wen Y, Gou R, Wang Y, Xu Q. The experimental therapy on brain ischemia by improvement of local angiogenesis with tissue engineering in the mouse. Cell Transplant. 2014;23 Suppl 1:S83-95.

[10] Pitaksuteepong T, Somsiri A, Waranuch N. Targeted transfollicular delivery of artocarpin extract from Artocarpus incisus by means of microparticles. European journal of pharmaceutics and biopharmaceutics : official journal of Arbeitsgemeinschaft fur Pharmazeutische Verfahrenstechnik eV. 2007;67:639-45.

[11] Tuladhar A, Morshead CM, Shoichet MS. Circumventing the blood-brain barrier: Local delivery of cyclosporin A stimulates stem cells in stroke-injured rat brain. Journal of controlled release : official journal of the Controlled Release Society. 2015;215:1-11.

[12] Zhu S, Nih L, Carmichael ST, Lu Y, Segura T. Enzyme-Responsive Delivery of Multiple Proteins with Spatiotemporal Control. Adv Mater. 2015;27:3620-5.

[13] Lam J, Lowry WE, Carmichael ST, Segura T. Delivery of iPS-NPCs to the Stroke Cavity within a Hyaluronic Acid Matrix Promotes the Differentiation of Transplanted Cells. Adv Funct Mater. 2014;24:7053-62.

[14] Chai C, Leong KW. Biomaterials approach to expand and direct differentiation of stem cells. Mol Ther. 2007;15:467-80.

[15] Moshayedi P, Carmichael ST. Hyaluronan, neural stem cells and tissue reconstruction after acute ischemic stroke. Biomatter. 2013;3.

[16] Hanjaya-Putra D, Wong KT, Hirotsu K, Khetan S, Burdick JA, Gerecht S. Spatial control of cell-mediated degradation to regulate vasculogenesis and angiogenesis in hyaluronan hydrogels. Biomaterials. 2012;33:6123-31.

[17] Michalski D, Hartig W, Krueger M, Hobohm C, Kas JA, Fuhs T. A novel approach for mechanical tissue characterization indicates decreased elastic strength in brain areas affected by experimental thromboembolic stroke. Neuroreport. 2015;26:583-7.

[18] Lowry WE, Richter L, Yachechko R, Pyle AD, Tchieu J, Sridharan R, et al. Generation of human induced pluripotent stem cells from dermal fibroblasts. Proc Natl Acad Sci U S A. 2008;105:2883-8.

[19] Karumbayaram S, Novitch BG, Patterson M, Umbach JA, Richter L, Lindgren A, et al. Directed differentiation of human-induced pluripotent stem cells generates active motor neurons. Stem Cells. 2009;27:806-11.

[20] Lei Y, Gojgini S, Lam J, Segura T. The spreading, migration and proliferation of mouse mesenchymal stem cells cultured inside hyaluronic acid hydrogels. Biomaterials. 2011;32:39-47.

[21] Lam J, Carmichael ST, Lowry WE, Segura T. Hydrogel design of experiments methodology to optimize hydrogel for iPSC-NPC culture. Advanced healthcare materials. 2015;4:534-9.

[22] Harilall SL, Choonara YE, Tomar LK, Tyagi C, Kumar P, du Toit LC, et al. Development and in vivo evaluation of an implantable nano-enabled multipolymeric scaffold for the management of AIDS dementia complex (ADC). International journal of pharmaceutics. 2015.

[23] Clarkson AN, Huang BS, Macisaac SE, Mody I, Carmichael ST. Reducing excessive GABA-mediated tonic inhibition promotes functional recovery after stroke. Nature. 2010;468:305-9.

[24] Lin SZ, Chiou AL, Wang Y. Ketamine antagonizes nitric oxide release from cerebral cortex after middle cerebral artery ligation in rats. Stroke. 1996;27:747-52.

[25] Christ AF, Franze K, Gautier H, Moshayedi P, Fawcett J, Franklin RJ, et al. Mechanical difference between white and gray matter in the rat cerebellum measured by scanning force microscopy. Journal of biomechanics. 2010;43:2986-92.

[26] Harrison RH, St-Pierre JP, Stevens MM. Tissue engineering and regenerative medicine: a year in review. Tissue engineering Part B, Reviews. 2014;20:1-16.

[27] Baffert F, Le T, Sennino B, Thurston G, Kuo CJ, Hu-Lowe D, et al. Cellular changes in normal blood capillaries undergoing regression after inhibition of VEGF signaling. American journal of physiology Heart and circulatory physiology. 2006;290:H547-59.

[28] Binder DK, Scharfman HE. Brain-derived neurotrophic factor. Growth factors. 2004;22:123-31.

[29] Steinbeck JA, Studer L. Moving stem cells to the clinic: potential and limitations for brain repair. Neuron. 2015;86:187-206.

[30] Anderson SM, Chen TT, Iruela-Arispe ML, Segura T. The phosphorylation of vascular endothelial growth factor receptor-2 (VEGFR-2) by engineered surfaces with electrostatically or covalently immobilized VEGF. Biomaterials. 2009;30:4618-28.

[31] Couillard-Despres S, Winner B, Schaubeck S, Aigner R, Vroemen M, Weidner N, et al. Doublecortin expression levels in adult brain reflect neurogenesis. Eur J Neurosci. 2005;21:1-14.

[32] Pevny LH, Nicolis SK. Sox2 roles in neural stem cells. Int J Biochem Cell Biol. 2010;42:421-4.

[33] Svendsen CN, Bhattacharyya A, Tai YT. Neurons from stem cells: preventing an identity crisis. Nat Rev Neurosci. 2001;2:831-4.

[34] Park H, Poo MM. Neurotrophin regulation of neural circuit development and function. Nat Rev Neurosci. 2013;14:7-23.

[35] Moon BS, Yoon JY, Kim MY, Lee SH, Choi T, Choi KY. Bone morphogenetic protein 4 stimulates neuronal differentiation of neuronal stem cells through the ERK pathway. Experimental & molecular medicine. 2009;41:116-25.

[36] Khakh BS, Sofroniew MV. Diversity of astrocyte functions and phenotypes in neural circuits. Nat Neurosci. 2015;18:942-52.

[37] Kelly S, Bliss TM, Shah AK, Sun GH, Ma M, Foo WC, et al. Transplanted human fetal neural stem cells survive, migrate, and differentiate in ischemic rat cerebral cortex. Proc Natl Acad Sci U S A. 2004;101:11839-44.

[38] Carmichael ST. Cellular and molecular mechanisms of neural repair after stroke: making waves. Annals of neurology. 2006;59:735-42.

[39] Chapman AR, Scala CC. Evaluating the first-in-human clinical trial of a human embryonic stem cell-based therapy. Kennedy Institute of Ethics journal. 2012;22:243-61.

[40] Fuhrmann T, Tam RY, Ballarin B, Coles B, Elliott Donaghue I, van der Kooy D, et al. Injectable hydrogel promotes early survival of induced pluripotent stem cell-derived oligodendrocytes and attenuates longterm teratoma formation in a spinal cord injury model. Biomaterials. 2016;83:23-36.

[41] Zhang J, Tokatlian T, Zhong J, Ng QK, Patterson M, Lowry WE, et al. Physically associated synthetic hydrogels with long-term covalent stabilization for cell culture and stem cell transplantation. Adv Mater. 2011;23:5098-103.

[42] Lim TC, Toh WS, Wang LS, Kurisawa M, Spector M. The effect of injectable gelatin-hydroxyphenylpropionic acid hydrogel matrices on the proliferation, migration, differentiation and oxidative stress resistance of adult neural stem cells. Biomaterials. 2012;33:3446-55.

[43] Wang TY, Bruggeman KF, Kauhausen JA, Rodriguez AL, Nisbet DR, Parish CL. Functionalized composite scaffolds improve the engraftment of transplanted dopaminergic progenitors in a mouse model of Parkinson's disease. Biomaterials. 2016;74:89-98.

[44] Leipzig ND, Wylie RG, Kim H, Shoichet MS. Differentiation of neural stem cells in three-dimensional growth factor-immobilized chitosan hydrogel scaffolds. Biomaterials. 2011;32:57-64.

[45] Cheng TY, Chen MH, Chang WH, Huang MY, Wang TW. Neural stem cells encapsulated in a functionalized self-assembling peptide hydrogel for brain tissue engineering. Biomaterials. 2013;34:2005-16.

[46] Ballios BG, Cooke MJ, Donaldson L, Coles BL, Morshead CM, van der Kooy D, et al. A Hyaluronan-Based Injectable Hydrogel Improves the Survival and Integration of Stem Cell Progeny following Transplantation. Stem Cell Reports. 2015;4:1031-45.

[47] Akhlaq M, Arshad MS, Mudassir AM, Hussain A, Kucuk I, Haj-Ahmad R, et al. Formulation and evaluation of anti-rheumatic dexibuprofen transdermal patches: a quality-by-design approach. Journal of drug targeting. 2015:1-27.

[48] Kauffman KJ, Dorkin JR, Yang JH, Heartlein MW, DeRosa F, Mir FF, et al. Optimization of Lipid Nanoparticle Formulations for mRNA Delivery in Vivo with Fractional Factorial and Definitive Screening Designs. Nano letters. 2015;15:7300-6.

[49] Hude RU, Jagdale SC. Optimization of Time Controlled 6-Mercaptopurine Delivery for Site-Specific Targeting to Colon Diseases. Current drug delivery. 2015.

[50] Al-Mahallawi AM, Khowessah OM, Shoukri RA. Nano-transfersomal ciprofloxacin loaded vesicles for non-invasive trans-tympanic ototopical delivery: in-vitro optimization, ex-vivo permeation studies, and in-vivo assessment. International journal of pharmaceutics. 2014;472:304-14.

[51] Gaudel C, Nongonierma AB, Maher S, Flynn S, Krause M, Murray BA, et al. A whey protein hydrolysate promotes insulinotropic activity in a clonal pancreatic beta-cell line and enhances glycemic function in ob/ob mice. J Nutr. 2013;143:1109-14.

[52] Mehanna MM, Alwattar JK, Elmaradny HA. Optimization, physicochemical characterization and in vivo assessment of spray dried emulsion: A step toward bioavailability augmentation and gastric toxicity minimization. International journal of pharmaceutics. 2015.

[53] Juhas M, Bursac N. Engineering skeletal muscle repair. Current opinion in biotechnology. 2013;24:880-6.

[54] Nih LR, Moshayedi P, Llorente IL, Berg AR, Cinkornpumin J, Lowry3, Segura T, Carmichael ST. Engineered HA hydrogel for stem cell transplantation in the brain: a design of experiment approach for an optimal biocompatibility. Biomaterials. In press

Figure Caption

Figure 1. Mechanical and composition gel optimization (A) Schematic illustration of the injectable hyaluronic acid (HA) composed of acrylated hyaluronic acid, MMP degradable or non-degradable motifs, adhesion peptides and heparin bound growth factors. (B) Characterization of stiffness and crosslinker. (B*i*) Schematic illustration of brain coronal sections and their orientations. The stroke cavity is represented by the asterisk. (B*ii*, B*iii*) TTC-stained brain sections showing infarcted tissue (delimitated by dotted line) without (B*ii*) and with (B*iii*) injection of a 350 Pa gel in the stroke cavity. (B*iv*, B*v*) Vascular laminin staining (green) in HA gel (red) at 2 weeks post-injection with an MMP insensitive (or MMP-In; B*iv*) or sensitive (or MMP-Sen; B*v*) cross-linker. (B*vi*) Quantification of gel volume, (B*vii*) infarcted tissue and (B*viii*) the vascular density in the injected HA gels. DOE approach to optimize concentrations of (C) soluble or (D) bound growth factors. *iPS*-NPCs survival in HA gel at 1 week in response to varying concentrations of (C*i*) soluble or (D*i*) bound growth factors. DOE prediction for the maximized and minimized cell proliferation for (C*ii*) soluble and (D*ii*) bound growth factors. (E) Combining optimal growth factor concentrations. (E*i*) iPS-NPCs survival, (E*ii*) sprouting (Dcx staining) and (E*iii*, E*iv*) differentiation (% of Dcx cells by flow cytometry) in the combined optimization HA Max and HA Min at 1 week. (F) Schematics of the final optimized condition for *in vivo* testing and table of the gel component concentration. HA Nopt demonstrates non-optimized gel with equimolar concentrations of adhesion motifs and no GFs. Scale bars represent 1 mm (B*ii,* B*iii*), 100 µm (B*iv*, B*v*) and 50 µm (E*iv*). *, ** and *** indicate P < 0.05, P < 0.01 and P < 0.001, respectively.

Figure 2. Biomaterial infiltration and resorption *in vivo*. Fluorescent image of stroke area (A) 2 weeks and (B) 6 weeks after transplantation with 100,000 iPS-NPCs (green) encapsulated in HA Max (blue), or (C) 6 weeks after transplantation of 50,000 iPS-NPCs encapsulated in HA Max. (D) Brain MRI images of animals at 9 weeks after stroke (dashed rectangle), (E) stroke plus HA Max injection and (F) stroke plus transplantation of 100,000 cells encapsulated in HA Max. (J) Quantification of gel representing T2 signal (arrowhead in E and F). (K) Fluorescent staining of vascular growth within HA Max at two weeks after transplantation, where the area demarcated in dashed line is magnified in L (merged), M (transplanted cells, in green), N (CD31 positive

endothelial cells, in red) and O (gel, in blue). Scale bar represents 100 µm (A-C) and 10 µm (K-H). ** indicates P < 0.01.

Figure 3. Cell proliferation, differentiation and survival in HA gel. (A) Fluorescent image and (B) analyses of brain sections injected with 100,000 cells stained at 2 weeks for the human-specific nuclear antigen HuNu and the proliferation marker Ki67, and at 6 weeks for HuNu, GFP, the neural precursor marker SOX2 and the neuronal antigen NF200. (C) Survival of transplanted cells with and without prior encapsulation was analyzed at 2 weeks post-injection on brain section stained for GFP. Ratio of GFP positive area was quantified in each group. Scale bars represents 25 µm (A) and 200 µm (C). * indicates P < 0.05.

Figure 4. Effect of HA Max composition on astrocytic cell differentiation. (A) Fluorescent images and (B) analyses of brain sections injected with 100,000 cells stained at 6 weeks for GFP, GFAP, as the marker for both astrocytes and NPCs, and S100b that is more specific to astrocytes. The numbers of GFP/GFAP as well as GFP/GFAP/S100b positive cells were normalized to the total GFP cells to obtain a percentage cells expressing one or both astrocytic markers. In addition, triple labeled cells were normalized to the number of GFP-GFAP cells in order to estimate the percentage of GFAP cells that are also positive for the more exclusive astrocytic marker, S100b. Scale bars, 50 µm. **** indicates P < 0.0001.
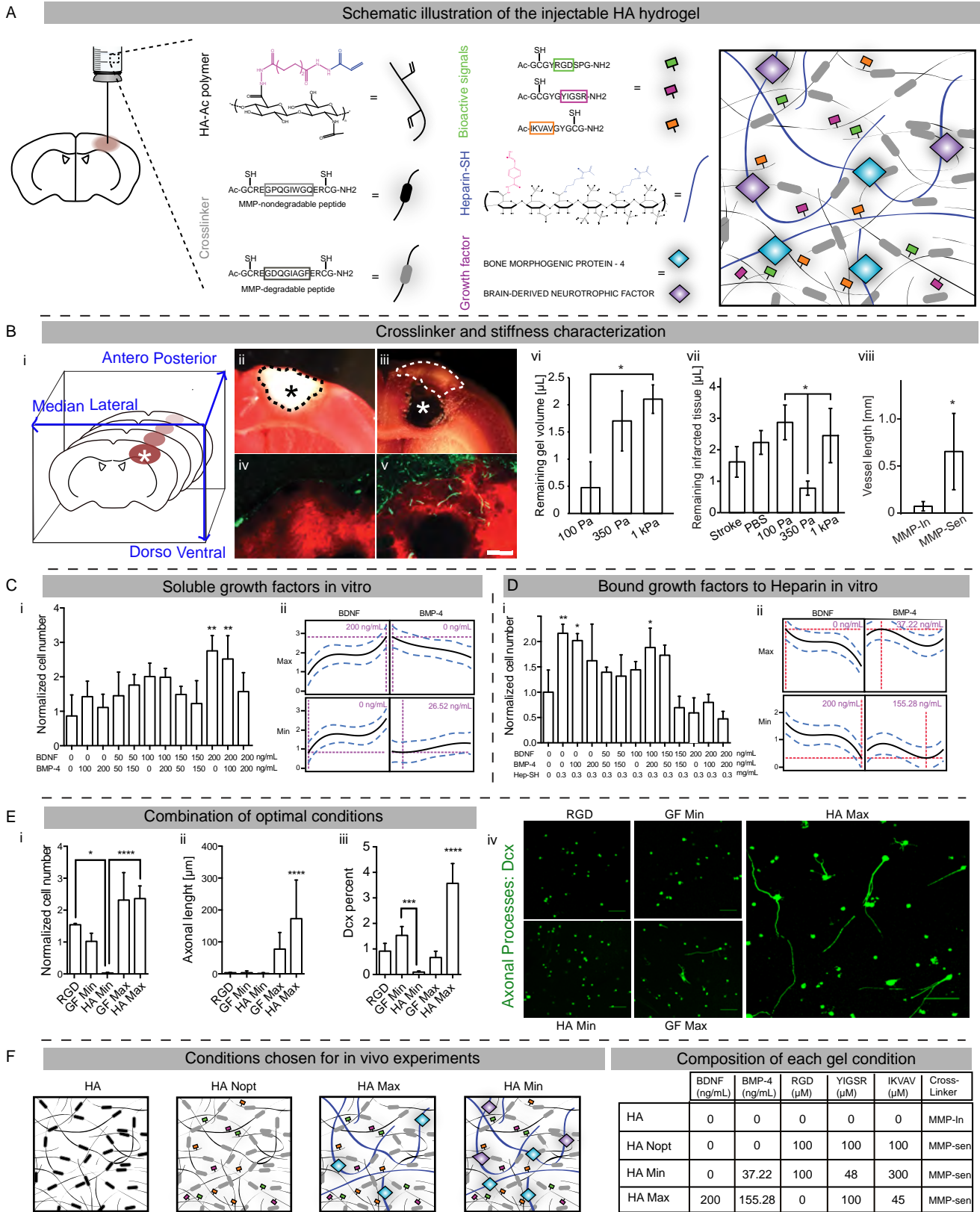
Figure 1

A — Schematic illustration of the injectable HA hydrogel

HA-Ac polymer

Crosslinker

Bioactive signals

Ac-GCGY RGD SPG-NH2

Ac-GCGYG YIGSR -NH2

Ac- IKVAV GYGCG-NH2

Heparin-SH

Growth factor

SH

Ac-GCRE GPQGIWGQ ERCG-NH2
MMP-nondegradable peptide

SH

Ac-GCRE GDQGIAGF ERCG-NH2
MMP-degradable peptide

BONE MORPHOGENIC PROTEIN - 4

BRAIN-DERIVED NEUROTROPHIC FACTOR

B — Crosslinker and stiffness characterization

i — Antero Posterior / Median Lateral / Dorso Ventral

vi — Remaining gel volume [µL] — 100 Pa, 350 Pa, 1 kPa

vii — Remaining infarcted tissue [µL] — Stroke, PBS, 100 Pa, 350 Pa, 1 kPa

viii — Vessel length [mm] — MMP-In, MMP-Sen

C — Soluble growth factors in vitro

i — Normalized cell number

| BDNF | 0 | 0 | 0 | 50 | 50 | 100 | 100 | 150 | 150 | 200 | 200 | 200 | ng/mL |
| BMP-4 | 0 | 100 | 200 | 50 | 150 | 0 | 200 | 50 | 150 | 0 | 100 | 200 | ng/mL |

ii — BDNF / BMP-4 — Max: 200 ng/mL, 0 ng/mL; Min: 0 ng/mL, 26.52 ng/mL

D — Bound growth factors to Heparin in vitro

i — Normalized cell number

BDNF	0	0	0	0	50	50	100	100	150	150	200	200	200	ng/mL
BMP-4	0	0	100	200	50	150	0	200	50	150	0	100	200	ng/mL
Hep-SH	0	0.3	0.3	0.3	0.3	0.3	0.3	0.3	0.3	0.3	0.3	0.3	0.3	mg/mL

ii — BDNF / BMP-4 — Max: 0 ng/mL, 37.22 ng/mL; Min: 200 ng/mL, 155.28 ng/mL

E — Combination of optimal conditions

i — Normalized cell number — RGD, GF Min, HA Min, GF Max, HA Max

ii — Axonal lenght [µm] — RGD, GF Min, HA Min, GF Max, HA Max

iii — Dcx percent — RGD, GF Min, HA Min, GF Max, HA Max

iv — Axonal Processes: Dcx — RGD, GF Min, HA Max, HA Min, GF Max

F — Conditions chosen for in vivo experiments

HA, HA Nopt, HA Max, HA Min

Composition of each gel condition

	BDNF (ng/mL)	BMP-4 (ng/mL)	RGD (µM)	YIGSR (µM)	IKVAV (µM)	Cross-Linker
HA	0	0	0	0	0	MMP-In
HA Nopt	0	0	100	100	100	MMP-sen
HA Min	0	37.22	100	48	300	MMP-sen
HA Max	200	155.28	0	100	45	MMP-sen

Figure 2

HA Max + 100,000 cells at 2 weeks | **HA Max + 100,000 cells at 6 weeks** | **HA Max + 50,000 cells at 6 weeks**

iPS-NPCs / HA Gel

A   B   C

No HA at 9 weeks | **HA Max at 9 weeks** | **HA Max, 100,000 cells at 9 weeks** | **HA Max at 9 weeks**

MRI

D   E   F   J

Remaining gel Vol (uL)

HA Max   HA Max+cells

**

HA Max + 100,000 cells at 2 weeks

iPS-NPCs / HA Gel / Vessels: CD31

K   L   M   N   O

Figure 3

Figure 4